Theor Appl Genet (2012) 124:623–635
DOI 10.1007/s00122-011-1734-1

ORIGINAL PAPER

Towards the adaptation of grapevine varieties to climate change: QTLs and candidate genes for developmental stages

Eric Duchêne · Gisèle Butterlin · Vincent Dumas · Didier Merdinoglu

Received: 24 May 2011 / Accepted: 14 October 2011 / Published online: 4 November 2011
© Springer-Verlag 2011

Abstract The genetic determinism of developmental stages in grapevine was studied in the progeny of a cross between grapevine cultivars Riesling and Gewurztraminer by combining ecophysiological modelling, genetic analysis and data mining of the grapevine whole genome sequence. The dates of three phenological stages, budbreak, flowering and veraison, were recorded during four successive years for 120 genotypes in the vineyard. The phenotypic data analysed were the duration of three periods expressed in thermal time (degree-days): 15 February to budbreak (Bud), budbreak to flowering (Flo) and flowering to veraison (Ver). Parental and consensus genetic maps were built using 153 microsatellite markers on 188 individuals. Six independent quantitative trait loci (QTLs) were detected for the three phases. They were located on chromosomes 4 and 19 for Bud, chromosomes 7 and 14 for Flo and chromosomes 16 and 18 for Ver. Interactions were detected between loci and also between alleles at the same locus. Using the available grapevine whole-genome sequences, candidate genes underlying the QTLs were identified. *VvFT*, on chromosome 7, and a *CONSTANS*-like gene, on chromosome 14, were found to colocalise with the QTLs for flowering time. Genes related to the abscisic acid response and to sugar metabolism were detected within the confidence intervals of QTLs for veraison time. Their possible roles in the developmental process are discussed. These results raise new hypotheses for a better understanding of the physiological processes governing grapevine phenology and provide a framework for breeding new varieties adapted to the future predicted climatic conditions.

Communicated by C. Gebhardt.

Electronic supplementary material The online version of this article (doi:10.1007/s00122-011-1734-1) contains supplementary material, which is available to authorized users.

E. Duchêne (✉) · G. Butterlin · V. Dumas · D. Merdinoglu
UMR 1131 Santé de la Vigne et Qualité du Vin, INRA, Université de Strasbourg, 28, rue de Herrlisheim, BP 20507, 68021 Colmar, France
e-mail: duchene@colmar.inra.fr

Introduction

Adapting grapevine (*Vitis vinifera* L.) varieties to future climatic conditions is a major challenge for the forthcoming years. Most of the grapevines in the world are cultivated for wine production, and it is generally accepted that elevated temperatures can impair the quality of grapes and wines (Jones et al. 2005). Grape quality parameters, such as sugar content, acidity, colour and aroma content, are determined during the ripening phase. The grapevine developmental cycle can be described by three main phenological stages: (i) budbreak, which is the onset of vegetative growth; (ii) flowering, leading post-fertilisation to the formation of berries; and (iii) veraison, which is the onset of the ripening process. At veraison, berries undergo major changes, e.g., cell wall degradation, skin coloration, sugar accumulation and malic acid degradation. The dates of veraison partly depend on the budbreak and flowering dates, and they are key factors for determining the climatic conditions during the ripening process. An acceleration in the time required to reach key phenological stages during the last few decades has been reported for several grape-growing areas (Duchêne and Schneider 2005; Ramos et al. 2008; Soar et al. 2008). This trend is expected to continue with the projected increase of temperatures, and the ripening period is likely to occur under warmer conditions,

not only because of an earlier onset of ripening in the summer but also because of higher temperatures on the same calendar date (Duchêne et al. 2010). A possible adaptation for the current grape-growing areas is to grow varieties with a later ripening period than those currently used. Such varieties can be obtained from germplasm collections or through breeding processes. Current breeding programmes based on marker-assisted selection (MAS) (Di Gaspero and Cattonaro 2010) are increasingly efficient, as studies have identified quantitative trait loci (QTLs) for numerous traits (review in Martinez-Zapater et al. (2010)), including the resistance to fungal diseases (Bellin et al. 2009; Blasi et al. 2011; Marguerit et al. 2009), the aroma content of the berries (Battilana et al. 2009; Duchêne et al. 2009) and the timing of developmental stages (Costantini et al. 2008). The availability of grapevine whole-genome sequences (Jaillon et al. 2007; Velasco et al. 2007) also offers new opportunities to identify candidate genes and to better understand the molecular and physiological basis of traits of interest.

In this paper, we present a genetic analysis of the variability in the time required for grapevines to reach specific developmental stages using progeny from a cross between Riesling (RI) and Gewurztraminer (GW) varieties. We describe the genetic variability of the observed dates of the developmental cycle using an ecophysiological model based on the calculation of heat sums expressed in growing degree-days between (i) 15 February and budbreak, (ii) budbreak and flowering and (iii) flowering and veraison (Duchêne et al. 2010). Using a genetic map built with microsatellite markers, we show in this work that independent QTLs can be identified for these three phases. Based on the grapevine whole-genome sequences, we propose here candidate genes underlying these QTLs, and we suggest some metabolic pathways likely to play a role in the grapevine budbreak, flowering and veraison processes.

Materials and methods

Populations and experimental conditions

To study the genetic determinism of yield components, berry composition (sugar, acids, aromas) and developmental stages, we created and evaluated progeny from a cross between *V. vinifera* cv. Riesling (RI) clone 49 (female) and *V. vinifera* cv. Gewurztraminer (GW) clone 643 (male). These two varieties were chosen because they differ for the above traits; we then expected to observe segregations. Among 527 seedlings from the RI × GW cross, 188 were randomly chosen for the construction of a genetic map. Among this first subset, 120 genotypes were randomly chosen and grafted in 2002 onto the Couderc 161-49 rootstock. Ten plants per genotype were planted according to a randomised 5-block design in an experimental vineyard at Bergheim (48°21′N, 7°34′E) in 2003. The vines were trained according to the double Guyot system.

Phenotyping

The budbreak, flowering and veraison dates were calculated, after successive scorings, as the dates when 50% of buds, flowers and berries, respectively, reached the required stage. Budbreak stage corresponded to Stage C "green tip", as described by Baggiolini (1952). Evaluation for veraison was based on berry softening. Developmental stages were recorded for 3 blocks and 4 years (2006–2009), i.e., on three 2-plant plots per genotype and per year. Stages were not evaluated for two of the available five blocks because we hypothesised that observing four more plants per genotype would not significantly improve the evaluation of the traits. Heat sums were calculated in degree-days (dd) as proposed by Duchêne et al. (2010), with daily maximum temperatures and base temperatures of 2, 10 and 6°C for the "15 February to budbreak" (Bud), "budbreak to flowering" (Flo) and "flowering to veraison" (Ver) phases, respectively. A meteorological station next to the experimental plot provided temperature data.

Genotypic effects used for QTL detection were determined using analysis of variance with mixed models where the year, genotype × year interaction, and individual plot were considered random effects. Calculations were performed with the R software, version 2.10.0 (© R Foundation for Statistical Computing, 2009) with the lme4 package. Five datasets were used for QTL detection: one for each year (2006–2009) and one with the estimates of genotypic effects when the "year" effect was included as a random factor in the model of analysis of variance. The estimated values for this 4-year dataset are close to the mean of the four values from each year. Heritabilities of the interannual genotypic means were calculated as:

$$H = \frac{\sigma^2_G}{\sigma^2_G + \frac{\sigma^2_{GY}}{4} + \frac{\sigma^2_E}{12}}$$

where is σ^2_G is the genotypic variance, σ^2_{GY} is the genotype × year interaction variance and σ^2_E is the residual variance.

Simple sequence repeat (SSR) analysis

Genomic DNA extractions and methods for SSR analysis were performed as described by Merdinoglu et al. (2005). The sequences of the SSR primers used in this study can be

found in the NCBI UniSTS database (www.ncbi.nlm.nih.gov) except for VVC5 (Decroocq et al. 2003) and VVIm33 (Merdinoglu et al. 2005).

Electrophoregrams were analysed using Genescan™ 3.1 (Applied Biosystems, Foster City, USA). Alleles were identified using Genotyper™ 2.5.2 (Applied Biosystems, Foster City, USA), and their sizes were determined using the HD400-ROX internal size standard.

Construction of the genetic map

Genetic distances were calculated in Kosambi cM with the "R/qtl" package available for the R software (Broman et al. 2003). Parental maps were built considering only parental segregations, as in two backcrosses, and a consensus map was built on the basis of an ab × cd coding.

Marker orders were verified using the 'ripple' command, and the order with the minimal number of crossing-overs was chosen. When several marker orders were likely within a LOD 2 range, the order on the physical map (PN40024 line whole genome sequence, 12x release at http://www.genoscope.cns.fr/externe/GenomeBrowser/Vitis) was used as a reference.

QTL detection

QTL detection was performed on both parental and consensus maps with the R/qtl software (Broman et al. 2003) using the multiple imputation method ("`draws`" = 128) and the one-dimension scan command `scanone`. The two-dimension scan (`scantwo`) was used to search for interacting QTLs. LOD significances were ensured with permutation tests (1,000 permutations). QTL models were constructed step-by-step after the refinement of the QTL position (`refineqtl`), the search for supplementary QTLs (`addqtl`) and the search for interactions between QTLs (`addint`). The automatic detection procedure (`stepwiseqtl`, with a maximum of 5 QTLs) was also used after the calculation of LOD penalties. The LOD score and the percentage of variance explained by a QTL in a QTL model was assessed with analysis of variance using type III sums of squares (`fitqtl`). Confidence intervals were calculated as Bayesian credible intervals (`bayesesint`) with a probability of coverage of 0.95.

Analysis of variance (`lmer`) considering only data at marker positions but including all the phenotypic data (4 years, 3 blocks) was also used to confirm the results. The model of analysis of variance used for analysing the allelic effects at a locus L was as follows: $T_{ijk} = Y_i + B_j + LR_k + LG_k + G_k + P_{jk} + \varepsilon_{ijk}$, where T_{ijk} is the value of a given trait for the year i, block j and genotype k, LR_k is the effect of the alleles from RI at locus L (depending on the genotype of the individual k at this locus), LG_k is the effect of the alleles from GW at locus L (depending on the genotype of the individual k at this locus), G_k is the genotype background effect, P_{jk} is a single plot effect and ε_{ijk} is the residual error. Year, genotype background and plot were considered random effects. Interactions between markers were tested by introducing a term for the interactions in the model.

Significance of an effect in a model was assessed using a likelihood ratio, and associated P values based on a χ^2 distribution were confirmed with 1,000 simulations comparing models both with and without the tested fixed effect. In this paper, we use the system for QTL names proposed in the R/qtl software: chromosome@position (e.g., 14@59 for a QTL positioned at 59 cM on the genetic map of chromosome 14).

Determination of candidate genes for developmental stages

The Genoscope 12x whole genome sequence (WGS) release of the PN40024 line (http://www.genoscope.cns.fr/externe/GenomeBrowser/Vitis/; Jaillon et al. (2007)) was explored to search for candidate genes. When their accurate positions in the PN40024 genome release were unknown, the Pinot noir ENTAV 115 WGS (http://genomics.research.iasma.it/gb2/gbrowse/grape/; Velasco et al. (2007)) was used. The physical positions of our confidence intervals were assessed according to the physical positions of the microsatellite markers in the genome and to their position in our consensus map. In parallel, we searched for genes mentioned in the literature for their possible role in the genetic determinism of budbreak, flowering or onset of ripening, not only in grapevine but also in other perennial and annual species. Finally, we checked which of these genes were located within our confidence intervals.

Results

Segregations and heritabilities

Bud, Flo and Ver segregated in the progeny each year. The distributions were not skewed (Fig. 1) and no transformations were applied to the variables. Heritabilities of the genotypic means in the complete dataset were high, between 85 and 92% (Table 1). Values for Flo were similar for the two parents and close to the mean value observed in the progeny. Transgressions were observed, and the range of variations, approximately 70 dd, represents approximately 12% of the mean value. The parents differed more for the values of Bud and Ver. Particularly for Ver, RI was one of the latest genotypes. The variation among genotypes

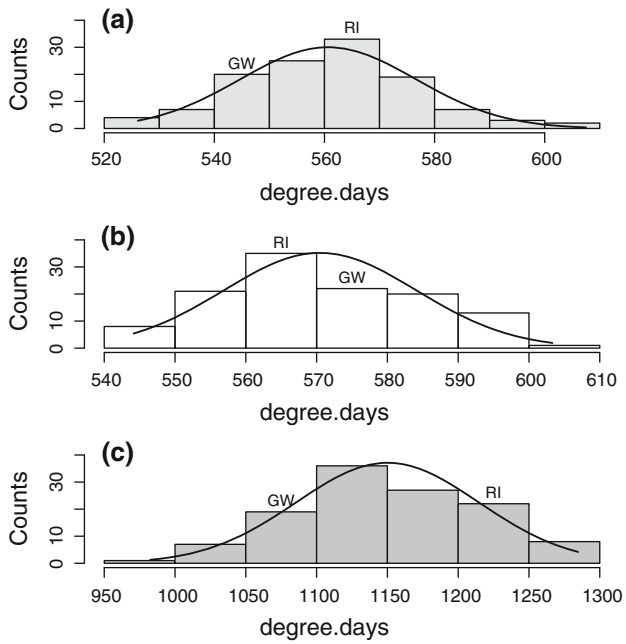

Fig. 1 Histogram of segregations of the genotypic effects (heat sums in degree-days over 4 years of data) in the RIxGW progeny. *Lines* represent the corresponding normal curves (mean and standard deviation of the progeny). **a** From 15 February to budbreak (Bud); **b** from budbreak to flowering (Flo); **c** from flowering to veraison (Ver). The class of the parents are indicated (*RI* Riesling, *GW* Gewurztraminer)

was approximately 350 dd, i.e., approximately 30% of the mean value.

Genetic map

A total of 277 SSR markers were tested on the Riesling and Gewurztraminer parents; 163 of them were selected based on their heterozygocity in at least one of the parents and for providing a good coverage of the grapevine genome whilst avoiding redundancy.

Ultimately, 153 markers were included in the consensus map, which covers 1,131.1 cM over the 19 expected linkage groups (LG). Only two markers, VMC9c1 (LG 14) and VVC5 (LG 16), showed a distortion of segregation that was significant at $P = 0.05$. The average distances between markers were approximately 25% shorter than those in the grapevine framework map by Doligez et al. (2006). This might be partly due to the use of different software for the map calculations (R/qtl vs. CarthaGene), but heterogeneity between recombination rates was also observed between the five populations used for the framework map (Doligez et al. 2006). Differences with our mapping population are then not surprising.

With a recombination rate similar to the framework map, we can estimate that our consensus map would cover 1,508 cM, i.e., 92% of the total length of the framework map (1,646.8 cM). In the Riesling parental map, 129 markers cover 1,135 cM, while in the Gewurztraminer parental map, 119 markers cover 992.7 cM. Complete maps are presented as Online resource 1.

QTL detection

QTLs detected at $P = 0.05$ genome-wide with interval mapping methods were included in QTL models and are presented in Table 2 and Fig. 2. Percentages of variance explained in Table 2 take into account the presence of the other QTLs, i.e., values are additive. The results were confirmed by analysis of variance using data from the complete dataset, with a model built using the closest marker to the QTL peak for the 4-year dataset (Table 3).

Two main QTLs were found for Bud on LG 4 and 19, explaining 11.9 and 12%, respectively, of the phenotypic variance observed in the 4-year dataset with the consensus map. Allelic variations of RI were responsible for the QTL on LG 4, whereas the QTL on LG 19 was due to the effects of allelic variations in GW. There was no evidence of significant interactions between loci (Table 2) or between alleles at a given locus (Table 3). In some of the datasets, QTLs on LG 6, 7, 10 and 14 were also identified (Table 2).

Two strong QTLs were identified for Flo on LG 7 and 14 and they explained 16.2 and 27.4%, respectively, of the phenotypic variance observed in the 4-year dataset with the consensus map. They were detected in at least three growing seasons. The QTL on LG 14 explained up to 38.6% of the phenotypic variance observed in the 4-year dataset with the RI map. Additional QTLs on LG 2, 6, 15 and 16 were occasionally detected (Table 2). A significant interaction between loci on LG 14 and LG 15 was detected

Table 1 Variance components and heritabilities of the interannual genotypic means for the heat sums calculated for the three periods

Period	Variable	Genotype	Year	Genotype × year	Plot	Residual	Heritability of the means
15 February to budbreak	Bud	219.9	2,746.9	72.2	28.3	258.2	0.85
Budbreak to flowering	Flo	161.2	496.7	29.3	9.2[a]	153.6	0.89
Flowering to veraison	Ver	3,773.6	332.7	924.4	389.1	1,083.7	0.92

All the random effects of this table were significant at $P = 0.001$ with a likelihood ratio test

[a] Significant only at $P = 0.05$

Table 2 Characteristics of the main QTLs detected in at least two different growing seasons and in the 4-year dataset

Period/variable	Linkage group	Map	Dataset	LOD Max	Associated marker	Confidence interval and LOD peak (cM)	% Var.	Other significant QTLs in the model
15 February–budbreak/Bud	4	RI	2006	2.8	VVIp37	26.0–56.2–56.2	9.9	14@59[a]
			2008	2.7	VrZAG21	12.0–30.0–50.0	10.1	
		Consensus	2006	4.8	VrZAG21	28.0–37.2–48.0	12.7	14@56, 19@42
			4-year	4.1	VrZAG21	26.0–38.0–54.0	11.9	7@72, 19@38
	19	GW	2006	3.7	VVIv33	36.0–44.0–48.0	14.1	
			4-year	2.8	VVIv33	26.0–42.0–48.0	8.3	6@44.7, 10@2
		Consensus	2006	6.7	VVIp34	36.0–42.0–48.0	18.7	4@37.2, 14@56
			2008	4.0	VVIp34	18.8–41.7–46.0	18.5	7@87.7
			4-year	5.5	VVIp34	30.0–38.0–44.0	12.0	4@38, 7@72
Budbreak–flowering/Flo	7	GW	2007	3.8	VMC8d11	44.0–50.0–68.0	12.2	6@20.7
			2008	5.8	VMC8d11	46.0–50.0–74.0	20.3	
			2009	3.8	VMC8d11	44.0–50.0–78.0	13.5	
			4-year	4.4	VMC8d11	46.0–50.0–72.0	15.8	
		Consensus	2007	6.9	VMC8d11	38.0–52.0–60.0	13.1	2@12, 6@8, 14@44
			2008	9.4	VMC8d11	52.0–56.7–68.0	22.6	14@38
			2009	5.2	VMC8d11	48.0–58.0–74.0	13.4	14@38
			4-year	8.0	VMC8d11	50.0–58.0–66.0	16.2	2@8, 14@38
	14	RI	2006	8.2	VVIn64	45.0–49.0–59.0	28.6	
			2007	7.9	VVMD24	39.0–45.0–51.0	24.7	15@36
			2008	7.7	VVMD24	37.0–47.0–53.0	23.6	16@44
			2009	7.5	VVMD24	36.0–46.0–51.0	25.1	
			4-year	14.2	VVMD24	45.0–47.0–49.0	38.6	15@17.4, 16@46, 14@47 × 15@17.4[b]
		Consensus	2006	12.3	VVIn64	42.0–48.0–59.0	28.0	
			2007	9.7	VVMD24	38.0–44.0–48.0	19.6	2@12, 6@8, 7@52
			2008	9.3	VVMD24	36.0–38.0–59.0	22.4	7@56.7
			2009	8.4	VVMD24	32.0–38.0–46.0	23.2	7@58
			4-year	12.3	VVMD24	36.0–38.0–48.0	27.4	2@8, 7@58
Flowering–veraison/Ver	16	RI	2008	3.3	VVMD37	30.0–44.0–45.0	8.9	14@21, 18@80
			4-year	3.2	VVMD37	30.0–44.0–47.3	9	14@21, 18@80
		Consensus	2006	5.6	VVMD37	34.0–40.0–50.0	16.4	18@82
			2008	5.3	VVMD37	36.0–42.0–50.0	14.8	18@82
			2009	6.5	VVMD5	40.0–48.0–52.0	20.6	14@34
			4-year	4.8	VVMD37	36.0–42.0–50.0	13.7	18@83.1
	18	RI	2006	4.9	VVIu04	20.0–49.2–55.0	16.5	7@65
			2007	5.2	VVIn16	75.0–81.4–85.0	18.2	
			2008	3.6	VVIn16	45.0–80.0–85.0	9.7	14@21, 16@44
			2009	3.7	VVIn16	55.0–81.4–90.0	13.4	
			4-year	3.2	VVIn16	45.2–80.0–85.0	8.7	14@21, 16@44
		Consensus	2006	4.6	VVIn16	4.0–82.0–86.3	13.2	16@40
			2007	5.6	VVIn16	78.0–83.1–88.0	19.6	
			2008	5.9	VVIn16	54.0–82.0–88.0	16.6	16@42
			4-year	5.6	VVIn16	60.0–83.1–88.0	16	16@42

[a] Chromosome @ position on the genetic map

[b] Interaction between loci

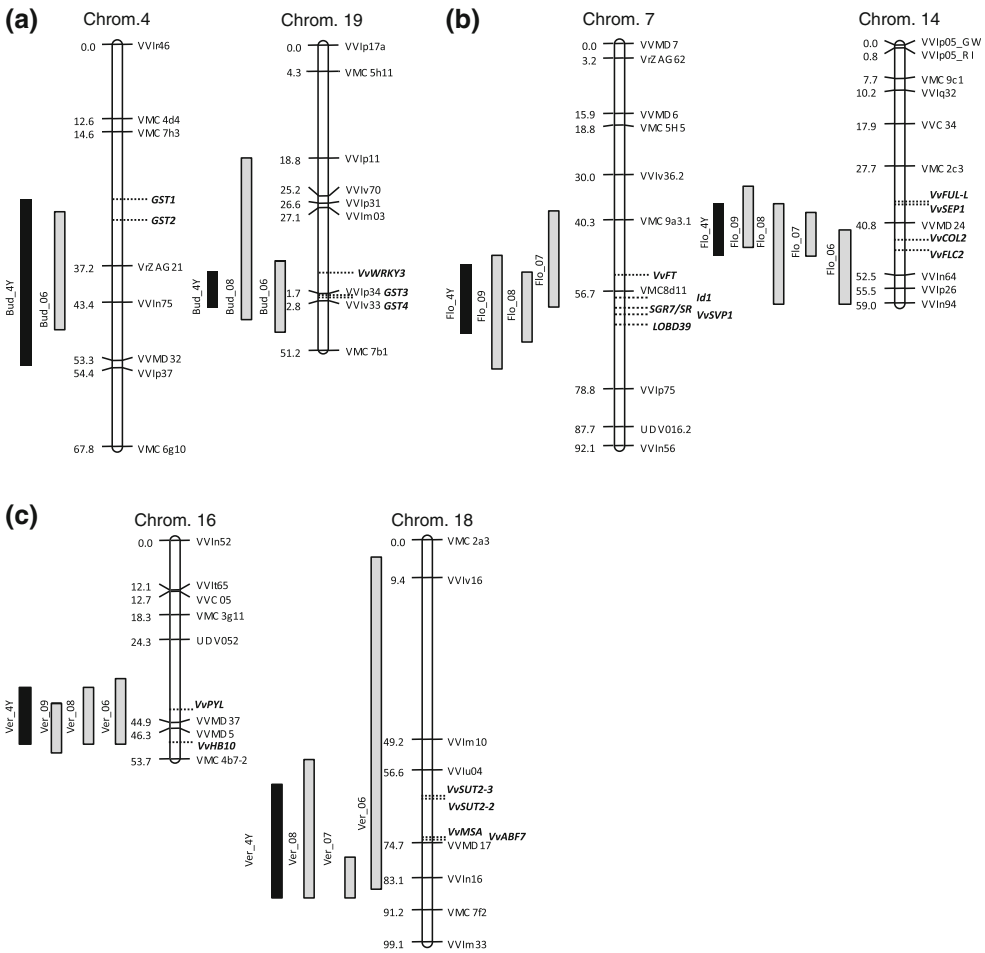

Fig. 2 Confidence intervals (Bayesian credible intervals, probability of coverage: 0.95) reported on the consensus map for different datasets (*4Y* = 4-year dataset in *black*, otherwise by year in *grey*). Candidate genes are positioned with *dashed lines*. Please refer to Table 5 for annotations. **a** QTLs for the length of the 15 February to budbreak period (*Bud*). **b** QTLs for the length of the budbreak to flowering period (*Flo*) **c** QTLs for the length of the flowering to veraison period (Ver)

in the 4-year dataset with the RI map (Table 2); the QTL at 14@47 had a strong effect, but the presence of allele 399 at VVIp33 had a negative effect on Flo when the genotype at 14@47 was A, whereas this effect was positive when the genotype at 14@47 was B (Fig. 3a). Moreover, alleles from RI and GW at the VMC8d11 locus on LG 7 also interacted with each other (Table 3; Fig. 3b); the effect of allele 136 from RI (+6.6 dd) was not significant when allele 136 from GW was present (interaction effect = −6.9 dd), whereas effects from RI alleles were significant in the context of the GW 132 allele.

Two QTLs for Ver were identified in the RI and in the consensus map on LG 16 and LG 18, where they explained 13.7 and 16%, respectively, of the phenotypic variance observed in the 4-year dataset with the consensus map (Table 2). An analysis of variance also detected significant effects for alleles from GW, although lower than for RI, as well as interactions between alleles from the two parents (Table 3). This interaction was very clear at VVMD37, where the greatest effect was observed when alleles 219 from RI and 217 from GW were combined (Fig. 4). Thus, effects from GW alleles were only significant when allele 219 from RI was present.

Candidate genes for developmental stages

The search for candidate genes was performed within the confidence intervals calculated in the consensus map for the 4-year dataset QTLs. The number of genes predicted in these confidence intervals varied from 93 (Flo, chromosome 7) to 292 (Ver, chromosome 18) (Table 4).

For budbreak, we focused on candidate genes proposed for other species or present in transcriptomics data on chilling requirements (Mathiason et al. 2009) or dormancy release (Ophir et al. 2009). Genes coding for glutathione *S*-transferase as well as a WRKY transcription factor were found in the confidence intervals: 2 on chromosome 4 and 3 on chromosome 19 (Table 5; Fig. 2a).

Nine genes linked to the flowering process were identified (Table 5; Fig. 2b). *VvFT*, on chromosome 7, belonged to the confidence intervals for all years. *VvCOL2*, on chromosome 14, was also within all of the confidence intervals.

The positions of grapevine genes participating in ethylene (Chervin and Deluc 2010; Chervin et al. 2008), auxin (Bottcher et al. 2010) or abscisic acid (Gambetta et al. 2010) signalling pathways were determined in the

Table 3 Analysis of variance with the closest markers to the detected QTLs

Period/variable	QTL[a]	Marker	Effect tested	Likelihood ratio test	*df*[b]	*P* value	Effect[c]
15 February–budbreak/Bud	4@38	VrZAG21	Alleles RI	16.8	2	<0.001	+11.3
			Alleles GW	1.2	2	ns	ns
			Interaction	1.0	1	ns	ns
	19@38	VVIp34	Alleles RI	1.7	2	ns	ns
			Alleles GW	16.9	2	<0.001	−10.9
			Interaction	1.7	1	ns	ns
Budbreak–flowering/Flo	7@8	VMC8d11	Alleles RI	6.1	2	0.04	6.6
			Alleles GW	29.6	2	<0.001	13.4
			Interaction	3.7	1	0.06[d]	−6.9
	14@47	VVMD24	Alleles RI	46.2	2	<0.001	13.9
			Alleles GW	1.2	2	ns	ns
			Interaction	0.3	1	ns	ns
Flowering–veraison/Ver	16@42	VVMD37	Alleles RI	13.6	2	<0.001	−9.7
			Alleles GW	8.4	2	0.02	−3.1
			Interaction	4.0	1	0.06[d]	−42.6
	18@83.1	VVIn16	Alleles RI	20.8	2	<0.001	47.1
			Alleles GW	3.5	2	ns	ns
			Interaction	2.0	1	ns	ns

[a] Chromosome @ position on the consensus map (4-year dataset)

[b] Degrees of freedom

[c] Difference between the estimates of the marker effects (allele B vs. allele A) expressed in degree-days. For an interaction, effect of the simultaneous presence of allele B from both parents

[d] $P < 0.001$ when the marker effect was tested as 4 independent levels of allelic combinations (AA, AB, BA and BB)

PN40024 line WGS. The effect of ABA on the onset of veraison has recently received increasing interest (Gambetta et al. 2010; Koyama et al. 2010; Owen et al. 2009; Wheeler et al. 2009), and the more relevant candidate genes detected in our confidence intervals are related to ABA and sugar signalling pathways (Table 5; Fig. 2c). A gene belonging to the recently discovered PYR/PYL family of ABA receptors colocalised with the QTL on chromosome 16, and an ABA stress and ripening-related (ASR) gene (*VvMSA*) colocalised with the QTL on chromosome 18.

Discussion

Our approach combined an ecophysiological model (Duchêne et al. 2010) and genetic tools. We chose to focus on the length of three important developmental periods, expressed in degree-days: Bud, Flo and Ver. This allowed us to detect independent QTLs for budbreak (LG 4 and 19), budbreak to flowering (LG 7 and 14) and flowering to veraison (LG 16 and 18). In our study, the "Year" and the "Genotype × Year" effects were significant, which means that our model has room for improvement. Ecophysiological models have been successful for analysing the genetic determinism of complex traits, such as fruit quality (Quilot et al. 2005) or tolerance to water stress (Reymond et al. 2003; Uptmoor et al. 2009). Detection of QTLs for phenology using models has also been reported for rice (Nakagawa et al. 2005) and barley (Yin et al. 2005).

Models allow a better dissection of a trait, and QTLs independent from environmental conditions are of particular interest for testing ideotypes. Quantitative allelic effects independent from environmental conditions can be used to predict the behaviour of genotypes for other geographical conditions and also for future climatic scenarios (Duchêne et al. 2010). Applied to the grapevine, this approach provides support to help determine which loci should be considered a priority in the breeding process.

To our knowledge, this is the first report of QTLs identified for budbreak in the grapevine. Two QTLs were detected, on LG 4 and 19, in 2006 and 2008. Together, they could explain up to 31.4% of the phenotypic variance in 2006. QTLs for budbreak can be associated with two physiological processes. Indeed, budbreak dates depend (i) on the date of dormancy release and (ii) on the positive response to temperatures after this date (see Garcia de Cortazar Atauri et al. (2009) for a review). Garcia de Cortazar Atauri et al. (2009) propose different values, in "chilling units", that are necessary for dormancy release

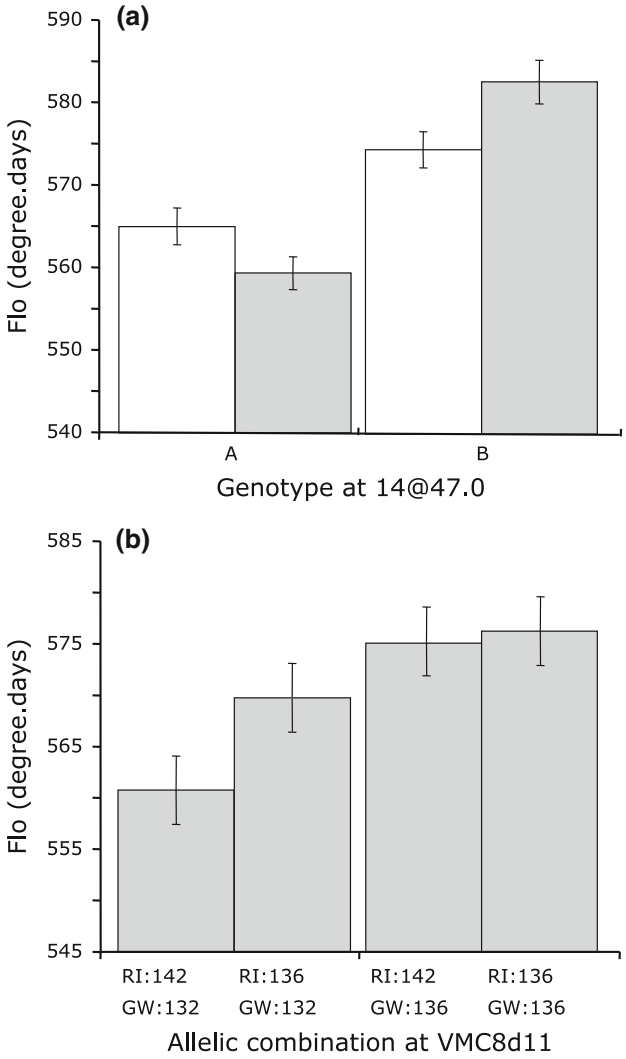

Fig. 3 Interactions on the length of the budbreak-flowering period (*Flo*, 4-year dataset). *Bars* represent standard errors. **a** between two loci (Riesling map). *White*, *grey* alleles 403 and 399 at VVIp33 (LG 15), respectively. Genotype at 14@47 in absence of recombination: *A* alleles 82 at VVIn64 and 217 at VVMD24, *B* alleles 70 at VVIn64 and 209 at VVMD24; **b** between alleles at VMC8d11 (LG 7)

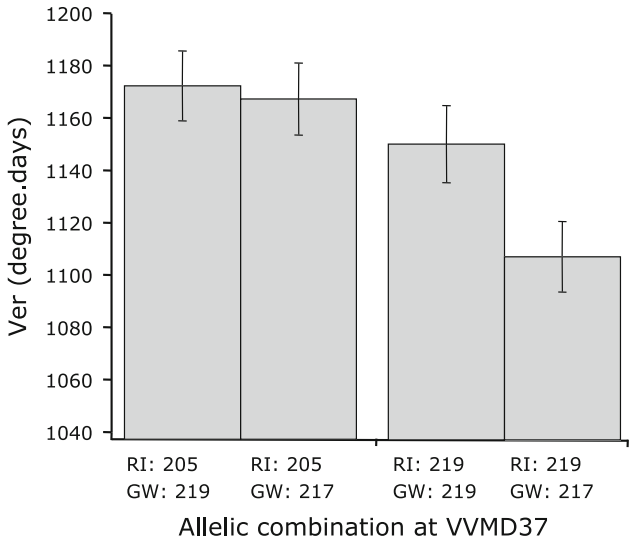

Fig. 4 Interactions between alleles at VVMD37 on the length of the flowering–veraison period (*Ver*, 4-year dataset). *Bars* represent standard errors

for different grapevine varieties. As the date of dormancy release is difficult to assess for a population containing 120 different genotypes, we have to assume that the chilling requirements were fulfilled at the time we started heat summations (15 February). This hypothesis is reasonable, as the latest date of chilling requirements predicted with the model of Garcia de Cortazar Atauri et al. (2009) for Riesling over the 4 years of our study was 17 December. However, in the present study, we cannot distinguish whether the heat sums calculated between 15 February and budbreak reflect differences in the dates of dormancy release or differences in the growth rates starting at the same date of dormancy release for all 120 genotypes.

A search for candidate genes involved in budbreak put forward genes coding for glutathione *S*-transferase (Table 5; Fig. 2a). An increase in the expression levels of such genes has been shown after hydrogen cyanamide (HCN) application, heat shock of the buds to release dormancy (Keilin et al. 2007; Ophir et al. 2009) and also after natural chilling requirements (Pacey-Miller et al. 2003). The activities of glutathione *S*-transferase are consistent with the oxidative stress associated with the dormancy release process (Ophir et al. 2009). An induction of these genes in relation with budbreak has also been observed in other species (Mazzitelli et al. 2007; Walton et al. 2009). Ophir et al. (2009) propose a cascade of events leading to dormancy release where the ethylene and ABA (abscisic acid) metabolism processes play a central role. A WRKY transcription factor, VvWRKY3 (Gambetta et al. 2010), was found within the confidence interval on chromosome 19 (Fig. 4). Interestingly, this transcription factor is similar to AtWRKY2 (At5g56270) (Gambetta et al. 2010), which has been shown to mediate ABA effects on seed germination in *Arabidopsis thaliana* (Jiang and Yu 2009).

Two QTLs associated with Flo were found on chromosomes 7 and 14 (Table 2; Fig. 2b). They are different from those detected by Costantini et al. (2008) for flowering time, which were on chromosomes 1, 2 and 6 in Italia × Big Perlon progeny. There are several meaningful candidate genes within the confidence intervals of the QTLs (Table 5; Fig. 2b).

On chromosome 7, *VvFT*, for Flowering locus T, is one of the more relevant candidate genes. Indeed, this gene has a central role in the flowering process in *A. thaliana*, where its protein acts as a long-range signal to promote flowering (Huang et al. 2005). Over-expression of *VvFT* also hastened flowering in *Arabidopsis* (Carmona et al. 2007; Sreekantan and Thomas 2006).

Table 4 Confidence intervals (CI) explored for candidate genes identification in the Genoscope 12x release of the PN40024 line genome sequence

Trait[a]	QTL on	Left marker	Right marker	Left limit of the CI (bp)	Right limit of the CI (bp)	Length of the CI (bp)	Number of genes in the CI
Bud	LG4	VrZAG21	VVIn75	11,525,084	16,833,861	5,308,777	145
	LG19	VVIp34	VVIv33	10,554,320	14,882,349	4,328,029	90
Flo	LG7	VMC9a3.1	VVIp75	14,614,644	15,701,093	1,086,449	93
	LG14	VVMD24	VVIn64	23,287,124	25,698,974	2,411,849	181
Ver	LG16	UDV052	VVMD5	18,431,382	21,631,537	3,200,156	218
	LG18	VVIu04	VVIn16	14,816,454	25,208,444	10,391,991	292

[a] For the 4-year dataset

VvSVP1, also located on chromosome 7, is encoding for a MIKC^{C}-Type MADS-box protein (Diaz-Riquelme et al. 2009). A homolog of *VvSVP1, JOINTLESS,* has been associated with a QTL of flowering in tomato (Jimenez-Gomez et al. 2007). The expression level of *VvSVP1* increases as the differentiation of the inflorescences progress in latent buds in the season preceding flowering (Diaz-Riquelme et al. 2009). In *Arabidopsis*, SVP protein acts as a repressor of *FT* via direct binding to the *FT* sequence (Lee et al. 2007b), and it mediates the effect of ambient temperature. The repressor effect of SVP on *FT* has also been demonstrated in Chinese cabbage (Lee et al. 2007a). *VvFT* and *VvSVP1* cooperate to regulate flowering in *Arabidopsis* and they are only 2 Mbp apart in the Pinot noir ENTAV 115 WGS. As SVP protein regulates *FT* gene expression, our case may indicate a QTL represented by multiple genes instead of the individual effects of *VvFT* or *VvSVP1* alone.

Finally, *SGR7/SHR*, *LOBD39* and *Id1* are genes on chromosome 7 with an expression profile that varies in response to the photoperiod (Sreekantan et al. 2010). They are related to the flowering transition or to meristem formation and patterning, but their role in the flowering process is less clear than the roles of *VvFT* or *VvSVP1*.

On chromosome 14, four candidate genes were identified in the confidence interval for Flo: *VvFUL-L*, *VvSEP1*, *VvFLC2* and *VvCOL2*. *VvFUL-L* is a MADS-box transcription factor belonging to the same family as *VvFUL* and *VvAP1* (Diaz-Riquelme et al. 2009). *VvFUL-L* could play a role both in flowering induction and in tendril development (Calonje et al. 2004; Diaz-Riquelme et al. 2009). *VvSEP1* expression is clearly associated with flower development (Diaz-Riquelme et al. 2009). SEP class genes (SEPALLATA) belong to the E class of the ABCDE model of flower development, where they participate in the specification of floral organs (Melzer et al. 2010). A possible role for *VvSEP1* could be to impact the speed of flower development. Both *VvFUL-L* and *VvSEP1* did not belong to confidence intervals during all 4 years of the study, and their implication in determining the flowering time has less support than for *VvFLC2* and *VvCOL2*.

The *FLC* (FLOWERING LOCUS C) gene is a MADS-box transcription factor gene. In *Arabidopsis*, FLC acts as a floral inhibitor by repressing the expression of genes, such as *FT* (Amasino and Michaels 2010). The *FLC* homologs detected in grapevine, *VvFLC1* and *VvFLC2*, have quite divergent sequences and different expression patterns with respect to *FLC* in *Arabidopsis* (Diaz-Riquelme et al. 2009). Their expression is associated with the development of inflorescence branch meristems, but it is low in flowers and is not related to the flowering transition as in *Arabidopsis*. The possible role of *VvFLC2* is unclear, although its implication in the flowering process makes sense.

In *Arabidopsis*, *CONSTANS* (*CO*) is a floral promoter gene involved in photoperiodism perception. CO protein accumulates during long days and activates the expression of *FT* (Amasino and Michaels 2010). Two *CONSTANS* homologs have been characterised in grapevine (Almada et al. 2009): *VvCOL1* is localised on chromosome 4 and *VvCO* is localised on chromosome 14, but they are outside our 4-year confidence interval (22,695,812 bp to 22,698,379 bp). We have detected another *CONSTANS*-like gene that we named *VvCOL2*. CONSTANS-like proteins (GenBank accessions ADA54554/ADA54555) were found to be associated with genetic variations of flowering dates in *Medicago truncatula* (Pierre et al. 2010) and *Medicago sativa* (Herrmann et al. 2010). Similar proteins were identified on chromosomes 1 and 14 in the grapevine WGS: the predicted protein VvCOL2 on chromosome 14 in the Pinot noir ENTAV 115 WGS (glimmer.VV78X250837.10_4) is longer than that in the PN40024 line WGS (454 aa vs. 196 aa), has similarities with the *Arabidopsis* CONSTANS-like 14 protein (At2g33500 gene) and a convincing EST can be found in databases. These results indicate a possible role for *VvCOL2* in the flowering process.

A search for genes that could explain the genetic variations in veraison dates also yielded relevant candidates. On chromosome 16, *VvHB10* is a homeobox gene (class I HB transcription factor), similar to *AtHB7* and *AtHB12*

Table 5 Candidate genes underlying the identified QTLs

Related trait	Gene ID	Genome	Chrom.	Position	Gene symbol	Annotation	Reference for the annotation
Budbreak	GSVIVT01035262001	PN40024	4	11,587,680–11,589,305	*GST1*	Glutathione *S*-transferase	NCBI Blast on Swissprot
	GSVIVT01001479001	PN40024	4	12,133,777–12,135,719	*GST2*	Glutathione *S*-transferase	NCBI Blast on Swissprot
	GSVIVT01014953001	PN40024	19	12,826,742–12,829,288	*GST3*	Glutathione *S*-transferase	NCBI Blast on Swissprot
	GSVIVT01014963001	PN40024	19	13,089,548–13,090,890	*GST4*	Glutathione *S*-transferase	NCBI Blast on Swissprot
	GSVIVT01014854001	PN40024	19	10,665,036–10,669,055	VvWRKY3	WRKY transcription factor	Gambetta et al. (2010)
Flowering	GSVIVT01000107001	PN40024	7	15,325,228–15,327,698	*SGR7/SHR*	SHOOT GRAVITROPISM 7/SHORT-ROOT	Sreekantan et al. (2010)
	GSVIVT01000141001	PN40024	7	15,589,316–15,590,604	*LOBD39*	LOB domain-containing protein 39	Sreekantan et al. (2010)
	fgenesh.VV78X193757.4_1	Pinot N	7	16,134,566–16,136,821	*VvFT*	FLOWERING LOCUS T	Carmona et al. (2007)
	fgenesh.VV78X205200.8_1	Pinot N	7	17,334,104–17,335,492	*Id1*	INDETERMINATE 1	Sreekantan et al. (2010)
	fgenesh.VV78X111272.17_6	Pinot N	7	18,175,054–18,180,577	*VvSVP1*	SHORT VEGETATIVE PHASE/MADS-box protein JOINTLESS	Diaz-Riquelme et al. (2009) Jimenez-Gomez et al. (2007)
	GSVIVT01036549001	PN40024	14	23,320,331–23,341,234	*VvFUL-L*	FRUITFUL	Diaz-Riquelme et al. (2009)
	GSVIVT01036551001	PN40024	14	23,363,222–23,379,548	*VvSEP1*	SEPALLATA	Diaz-Riquelme et al. (2009)
	GSVIVT01033017001	PN40024	14	25,084,968–25,088,507	*VvCOL2*	CONSTANS-like protein	Herrmann et al. (2010)
	GSVIVT01033067001	PN40024	14	25,509,955–25,536,232	*VvFLC2*	FLOWERING LOCUS C	Diaz-Riquelme et al. (2009)
Veraison	GSVIVT01028704001	PN40024	16	19,636,837–19,641,201	*VvPYL*	ABA receptor PYL8	NCBI Blast on Swissprot
	GSVIVT01038619001	PN40024	16	21,439,501–21,441,052	*VvHB10*	Homeobox	Gambetta et al. (2010)
	GSVIVT01034886001	PN40024	18	15,923,474–15,926,074	*VvSUT2-2*	Putative sucrose sensor	Gambetta et al. (2010)
	GSVIVT01034881001	PN40024	18	15,866,681–15,868,604	*VvSUT2-3*	Putative sucrose sensor	Gambetta et al. (2010)
	GSVIVT01034540001	PN40024	18	19,680,342–19,687,518	*VvABF7*	ABRE-binding factor	Gambetta et al. (2010)
	NCBI Nucleotide DQ139800.1 No gene model in the PN40024 line genome 12x	PN40024	18	19,582,848–19,586,315	*VvMSA*	ASR, abscisic acid, stress and ripening-induced protein	Cakir et al. (2003)

(Gambetta et al. 2010). In *Arabidopsis*, the transcription of *AtHB7* is ABA-dependent (Olsson et al. 2004). Costantini et al. (2008) also identified a QTL for veraison time on chromosome 16, but our confidence interval does not cover this region (Fig. 2c); thus, it is likely that there are two QTLs for veraison time on this chromosome.

VvPYL, also on chromosome 16, is a more convincing candidate. ABA receptors have only recently been discovered (Kline et al. 2010), and *VvPYL* was identified in the grapevine WGS by similarity to genes of the *Arabidopsis* PYR/PYL family. The VvPYL-predicted protein shows 79% identity with the PYR1-like 8 protein from *Arabidopsis* (At5g53160 gene). ABA binds to PYR/PYL proteins, which in turn regulate a cascade of events, including the modification of phosphatase activities (for a review see Kline et al. (2010)). The regulation system is likely to be reversible and sensitive to ABA concentration gradients. As the presence of ABA in association with sugars induces ripening (Gambetta et al. 2010), VvPYL proteins could play a role in the genetic differences observed in veraison time in this study.

On chromosome 19, 4 genes related to ABA and sugar signalling were found. *VvSUT2-2* and *VvSUT2-3* have

homologies to both the *Arabidopsis* sucrose transporters (AtSUC1) and sucrose sensors (AtSUT2) (Gambetta et al. 2010). Both ABA and sugars are required to induce ripening (Gambetta et al. 2010), and the efficiency of sucrose transport or sucrose sensing could play a role in the triggering of veraison, but the actual mechanism may also lie elsewhere. *VvAB7F*, also located within our confidence interval on chromosome 19, is similar to the ABA-responsive transcription factor AtABI5 (Gambetta et al. 2010). In *Arabidopsis*, it has been proposed that the AtABI5 protein binds to the promoter of the sugar transporter *AtSUC1* (ortholog of *VvSUT2-2* and *VvSUT2-3* cf. *supra*) to regulate the expression of *AtSUC1* (Hoth et al. 2010). This example of crosstalk between ABA signalling and sugar metabolism is to be considered when trying to elucidate the determinism of veraison in grapevine. Cakir et al. (2003) have also described a similar mechanism in grapevine. These authors showed that a grapevine ASR protein was able to bind to two sugar-responsive elements in the promoter of the putative monosaccharide transporter *VvHT1*. The interesting point is that the gene coding for this ASR protein, *VvMSA*, was also identified within our confidence interval on chromosome 19. The study on crosstalks between ABA, stress and sugar signalling is an expanding research area (Hey et al. 2010; Kline et al. 2010). The presence of *VvSUT2-2*, *VvSUT2-3*, *VvABF7* and *VvMSA* in the chromosomic region of the QTL for veraison time suggest the presence of a complete pathway to regulate the sugar and ABA response at this locus. These results reinforce the hypothesis that the onset of ripening in grapevine is dependent on both sugar and ABA metabolism.

Conclusion

An ecophysiological model was used to characterise the genetic variability of budbreak, flowering and veraison dates in progeny from a Riesling × Gewurztraminer cross over four seasons. The joint analysis of these phenotypic data and of genetic variations at microsatellite loci allowed us to identify 6 independent QTLs: 2 for the 15 February to budbreak period on chromosomes 4 and 19; 2 for the budbreak to flowering period on chromosomes 7 and 14; and 2 for the flowering to veraison period on chromosomes 16 and 18. Interactions were detected between loci and also between alleles at the same locus. Relevant candidate genes were found in the confidence intervals of these QTLs by examining the available whole-genome sequences. *VvFT*, on chromosome 7, and a *CONSTANS*-like gene on chromosome 14 were the more convincing candidate genes for the flowering process. Several genes participating in ABA and sugar metabolism were found to colocalise with QTLs for the veraison process, and one of them, *VvPYL*, is similar to ABA receptor genes. These candidate genes open new perspectives for future studies on the genetic determinism of phenological stages in grapevine. Exploring their roles further and quantifying the effects of their genetic variations with ecophysiological models will provide a valuable framework to imagine and virtually test ideotypes of grapevine under projected climatic conditions.

Acknowledgments This work was partially financed by the ERA-NET Plant Genomics Program (GRASP GRAPE WINE 072b).

References

Almada R, Cabrera N, Casaretto JA, Ruiz-Lara S, Villanueva EG (2009) *VvCO* and *VvCOL1*, two *CONSTANS* homologous genes, are regulated during flower induction and dormancy in grapevine buds. Plant Cell Rep 28:1193–1203

Amasino RM, Michaels SD (2010) The timing of flowering. Plant Physiol 154:516–520

Baggiolini M (1952) Les stades repères dans le développement annuel de la vigne et leur utilisation pratique. Rev Rom Agric Vitic 8:4–6

Battilana J, Costantini L, Emanuelli F, Sevini F, Segala C, Moser S, Velasco R, Versini G, Grando MS (2009) The 1-deoxy-D-xylulose 5-phosphate synthase gene co-localizes with a major QTL affecting monoterpene content in grapevine. Theor Appl Genet 118:653–669

Bellin D, Peressotti E, Merdinoglu D, Wiedemann-Merdinoglu S, Adam-Blondon AF, Cipriani G, Morgante M, Testolin R, Di Gaspero G (2009) Resistance to *Plasmopara viticola* in grapevine 'Bianca' is controlled by a major dominant gene causing localised necrosis at the infection site. Theor Appl Genet 120:163–176

Blasi P, Blanc S, Wiedemann-Merdinoglu S, Prado E, Rühl E, Mestre P, Merdinoglu D (2011) Construction of a reference linkage map of *Vitis amurensis* and genetic mapping of *Rpv8* a locus conferring resistance to grapevine downy mildew. Theor Appl Genet 123:43–53

Bottcher C, Keyzers RA, Boss PK, Davies C (2010) Sequestration of auxin by the indole-3-acetic acid-amido synthetase GH3-1 in grape berry (*Vitis vinifera* L.) and the proposed role of auxin conjugation during ripening. J Exp Bot 61:3615–3625

Broman KW, Wu H, Sen S, Churchill GA (2003) R/qtl: QTL mapping in experimental crosses. Bioinformatics 19:889–890

Cakir B, Agasse A, Gaillard C, Saumonneau A, Delrot S, Atanassova R (2003) A grape ASR protein involved in sugar and abscisic acid signaling. Plant Cell 15:2165–2180

Calonje M, Cubas P, Martinez-Zapater JM, Carmona MJ (2004) Floral meristem identity genes are expressed during tendril development in grapevine. Plant Physiol 135:1491–1501

Carmona MJ, Calonje M, Martinez-Zapater JM (2007) The FT/TFL1 gene family in grapevine. Plant Mol Biol 63:637–650

Chervin C, Deluc L (2010) Ethylene signalling receptors and transcription factors over the grape berry development: gene expression profiling. Vitis 49:129–136

Chervin C, Tira-umphon A, Terrier N, Zouine M, Severac D, Roustan JP (2008) Stimulation of the grape berry expansion by ethylene and effects on related gene transcripts, over the ripening phase. Physiol Plant 134:534–546

Costantini L, Battilana J, Lamaj F, Fanizza G, Grando MS (2008) Berry and phenology-related traits in grapevine (*Vitis vinifera* L.): from quantitative trait loci to underlying genes. BMC Plant Biol 8:38

Decroocq V, Fave MG, Hagen L, Bordenave L, Decroocq S (2003) Development and transferability of apricot and grape EST microsatellite markers across taxa. Theor Appl Genet 106:912–922

Di Gaspero G, Cattonaro F (2010) Application of genomics to grapevine improvement. Aust J Grape Wine Res 16:122–130

Diaz-Riquelme J, Lijavetzky D, Martinez-Zapater JM, Carmona MJ (2009) Genome-wide analysis of MIKC^{C}-Type MADS Box genes in grapevine. Plant Physiol 149:354–369

Doligez A, Adam-Blondon AF, Cipriani G, Di Gaspero G, Laucou V, Merdinoglu D, Meredith CP, Riaz S, Roux C, This P (2006) An integrated SSR map of grapevine based on five mapping populations. Theor Appl Genet 113:369–382

Duchêne E, Schneider C (2005) Grapevine and climatic changes: a glance at the situation in Alsace. Agron Sustain Dev 25:93–99

Duchêne E, Butterlin G, Claudel P, Dumas V, Jaegli N, Merdinoglu D (2009) A grapevine (*Vitis vinifera* L.) deoxy-D-xylulose synthase gene colocates with a major quantitative trait loci for terpenol content. Theor Appl Genet 118:541–552

Duchêne E, Huard F, Dumas V, Schneider C, Merdinoglu D (2010) The challenge of adapting grapevine varieties to climate change. Clim Res 41:193–204

Gambetta GA, Matthews MA, Shaghasi TH, McElrone AJ, Castellarin SD (2010) Sugar and abscisic acid signaling orthologs are activated at the onset of ripening in grape. Planta 232:219–234

Garcia de Cortazar Atauri I, Brisson N, Gaudillere JP (2009) Performance of several models for predicting budburst date of grapevine (*Vitis vinifera* L.). Int J Biometeorol 53:317–326

Herrmann D, Barre P, Santoni S, Julier B (2010) Association of a CONSTANS-LIKE gene to flowering and height in autotetraploid alfalfa. Theor Appl Genet 121:865–876

Hey SJ, Byrne E, Halford NG (2010) The interface between metabolic and stress signalling. Ann Bot 105:197–203

Hoth S, Niedermeier M, Feuerstein A, Hornig J, Sauer N (2010) An ABA-responsive element in the *AtSUC1* promoter is involved in the regulation of *AtSUC1* expression. Planta 232:911–923

Huang T, Bohlenius H, Eriksson S, Parcy F, Nilsson O (2005) The mRNA of the *Arabidopsis* gene *FT* moves from leaf to shoot apex and induces flowering. Science 309:1694–1696

Jaillon O, Aury JM, Noel B, Policriti A, Clepet C, Casagrande A, Choisne N, Aubourg S, Vitulo N, Jubin C, Vezzi A, Legeai F, Hugueney P, Dasilva C, Horner D, Mica E, Jublot D, Poulain J, Bruyere C, Billault A, Segurens B, Gouyvenoux M, Ugarte E, Cattonaro F, Anthouard V, Vico V, Del Fabbro C, Alaux M, Di Gaspero G, Dumas V, Felice N, Paillard S, Juman I, Moroldo M, Scalabrin S, Canaguier A, Le Clainche I, Malacrida G, Durand E, Pesole G, Laucou V, Chatelet P, Merdinoglu D, Delledonne M, Pezzotti M, Lecharny A, Scarpelli C, Artiguenave F, Pe ME, Valle G, Morgante M, Caboche M, Adam-Blondon AF, Weissenbach J, Quetier F, Wincker P (2007) The grapevine genome sequence suggests ancestral hexaploidization in major angiosperm phyla. Nature 449:U463–U465

Jiang WB, Yu DQ (2009) *Arabidopsis WRKY2* transcription factor mediates seed germination and postgermination arrest of development by abscisic acid. BMC Plant Biol 9:96

Jimenez-Gomez JM, Alonso-Blanco C, Borja A, Anastasio G, Angosto T, Lozano R, Martinez-Zapater JM (2007) Quantitative genetic analysis of flowering time in tomato. Genome 50:303–315

Jones GV, White MA, Cooper OR, Storchmann K (2005) Climate change and global wine quality. Clim Change 73:319–343

Keilin T, Pang X, Venkateswari J, Halaly T, Crane O, Keren A, Ogrodovitch A, Ophir R, Volpin H, Galbraith D, Or E (2007) Digital expression profiling of a grape-bud EST collection leads to new insight into molecular events during grape-bud dormancy release. Plant Sci 173:446–457

Kline KG, Sussman MR, Jones AM (2010) Abscisic acid receptors. Plant Physiol 154:479–482

Koyama K, Sadamatsu K, Goto-Yamamoto N (2010) Abscisic acid stimulated ripening and gene expression in berry skins of the Cabernet Sauvignon grape. Funct Integr Genomic 10:367–381

Lee JH, Park SH, Lee JS, Ahn JH (2007a) A conserved role of SHORT VEGETATIVE PHASE (SVP) in controlling flowering time of *Brassica* plants. BBA-Gene Regul Mech 1769:455–461

Lee JH, Yoo SJ, Park SH, Hwang I, Lee JS, Ahn JH (2007b) Role of *SVP* in the control of flowering time by ambient temperature in *Arabidopsis*. Gene Dev 21:397–402

Marguerit E, Boury C, Manicki A, Donnart M, Butterlin G, Nemorin A, Wiedemann-Merdinoglu S, Merdinoglu D, Ollat N, Decroocq S (2009) Genetic dissection of sex determinism, inflorescence morphology and downy mildew resistance in grapevine. Theor Appl Genet 118:1261–1278

Martinez-Zapater JM, Carmona MJ, Diaz-Riquelme J, Fernandez L, Lijavetzky D (2010) Grapevine genetics after the genome sequence: challenges and limitations. Aust J Grape Wine Res 16:33–46

Mathiason K, He D, Grimplet J, Venkateswari J, Galbraith D, Or E, Fennell A (2009) Transcript profiling in *Vitis riparia* during chilling requirement fulfillment reveals coordination of gene expression patterns with optimized bud break. Funct Integr Genomic 9:81–96

Mazzitelli L, Hancock RD, Haupt S, Walker PG, Pont SDA, McNicol J, Cardle L, Morris J, Viola R, Brennan R, Hedley PE, Taylor MA (2007) Co-ordinated gene expression during phases of dormancy release in raspberry (*Rubus idaeus* L.) buds. J Exp Bot 58:1035–1045

Melzer R, Wang YQ, Theissen G (2010) The naked and the dead: the ABCs of gymnosperm reproduction and the origin of the angiosperm flower. Semin Cell Dev Biol 21:118–128

Merdinoglu D, Butterlin G, Bevilacqua L, Chiquet V, Adam-Blondon AF, Decroocq S (2005) Development and characterization of a large set of microsatellite markers in grapevine (*Vitis vinifera* L.) suitable for multiplex PCR. Mol Breed 15:349–366

Nakagawa H, Yamagishi J, Miyamoto N, Motoyama M, Yano M, Nemoto K (2005) Flowering response of rice to photoperiod and temperature: a QTL analysis using a phenological model. Theor Appl Genet 110:778–786

Olsson A, Engström P, Söderman E (2004) The homeobox genes *ATHB12* and *ATHB7* encode potential regulators of growth in response to water deficit in *Arabidopsis*. Plant Mol Biol 55:663–677

Ophir R, Pang XQ, Halaly T, Venkateswari J, Lavee S, Galbraith D, Or E (2009) Gene-expression profiling of grape bud response to two alternative dormancy-release stimuli expose possible links between impaired mitochondrial activity, hypoxia, ethylene-ABA interplay and cell enlargement. Plant Mol Biol 71:403–423

Owen SJ, Lafond MD, Bowen P, Bogdanoff C, Usher K, Abrams SR (2009) Profiles of abscisic acid and its catabolites in developing Merlot grape (*Vitis vinifera*) berries. Am J Enol Vitic 60:277–284

Pacey-Miller T, Scott K, Ablett E, Tingey S, Ching A, Henry R (2003) Genes associated with the end of dormancy in grapes. Funct Integr Genomic 3:144–152

Pierre J-B, Bogard M, Herrmann D, Huyghe C, Julier B (2010) A *CONSTANS*-like gene candidate that could explain most of the genetic variation for flowering date in *Medicago truncatula*. Mol Breed 28:25–35

Quilot B, Kervella J, Génard M, Lescourret F (2005) Analysing the genetic control of peach fruit quality through an ecophysiological model combined with a QTL approach. J Exp Bot 422:3083–3092

Ramos MC, Jones GV, Martinez-Casasnovas JA (2008) Structure and trends in climate parameters affecting winegrape production in northeast Spain. Clim Res 38:1–15

Reymond M, Muller B, Leonardi A, Charcosset A, Tardieu F (2003) Combining quantitative trait loci analysis and an ecophysiological model to analyse the genetic variability of the responses of maize leaf growth to temperatures and water deficit. Plant Physiol 131:664–675

Soar CJ, Sadras VO, Petrie PR (2008) Climate drivers of red wine quality in four contrasting Australian wine regions. Aust J Grape Wine Res 14:78–90

Sreekantan L, Thomas MR (2006) *VvFT* and *VvMADS8*, the grapevine homologues of the floral integrators *FT* and *SOC1*, have unique expression patterns in grapevine and hasten flowering in *Arabidopsis*. Funct Plant Biol 33:1129–1139

Sreekantan L, Mathiason K, Grimplet J, Schlauch K, Dickerson JA, Fennell AY (2010) Differential floral development and gene expression in grapevines during long and short photoperiods suggests a role for floral genes in dormancy transitioning. Plant Mol Biol 73:191–205

Uptmoor R, Osei-Kwarteng M, Gurtler S, Stutzel H (2009) Modeling the effects of drought stress on leaf development in a *Brassica oleracea* doubled haploid population using two-phase linear functions. J Am Soc Hortic Sci 134:543–552

Velasco R, Zharkikh A, Troggio M, Cartwright DA, Cestaro A, Pruss D, Pindo M, Fitzgerald LM, Vezzulli S, Reid J, Malacarne G, Iliev D, Coppola G, Wardell B, Micheletti D, Macalma T, Facci M, Mitchell JT, Perazzolli M, Eldredge G, Gatto P, Oyzerski R, Moretto M, Gutin N, Stefanini M, Chen Y, Segala C, Davenport C, Dematte L, Mraz A, Battilana J, Stormo K, Costa F, Tao Q, Si-Ammour A, Harkins T, Lackey A, Perbost C, Taillon B, Stella A, Solovyev V, Fawcett JA, Sterck L, Vandepoele K, Grando SM, Toppo S, Moser C, Lanchbury J, Bogden R, Skolnick M, Sgaramella V, Bhatnagar SK, Fontana P, Gutin A, Van de Peer Y, Salamini F, Viola R (2007) A high quality draft consensus sequence of the genome of a heterozygous grapevine variety. PLoS ONE 2:e1326

Walton EF, Wu RM, Richardson AC, Davy M, Hellens RP, Thodey K, Janssen BJ, Gleave AP, Rae GM, Wood M, Schaffer RJ (2009) A rapid transcriptional activation is induced by the dormancy-breaking chemical hydrogen cyanamide in kiwifruit (*Actinidia deliciosa*) buds. J Exp Bot 60:3835–3848

Wheeler S, Loveys B, Ford C, Davies C (2009) The relationship between the expression of abscisic acid biosynthesis genes, accumulation of abscisic acid and the promotion of *Vitis vinifera* L. berry ripening by abscisic acid. Aust J Grape Wine Res 15:195–204

Yin X, Struik PC, van Eeuwijk FA, Stam P, Tang J (2005) QTL analysis and QTL-based prediction of flowering phenology in recombinant inbred lines of barley. J Exp Bot 56:967–976